



HAL
open science

First detection and absolute transition frequencies in the (3–0) band of D2

S. Kassi, H. Fleurbaey, A. Campargue

► **To cite this version:**

S. Kassi, H. Fleurbaey, A. Campargue. First detection and absolute transition frequencies in the (3–0) band of D2. *The Journal of Chemical Physics*, 2024, 160 (9), 10.1063/5.0196903 . hal-04622185

HAL Id: hal-04622185


<https://hal.science/hal-04622185v1>

Submitted on 7 Nov 2024

HAL is a multi-disciplinary open access archive for the deposit and dissemination of scientific research documents, whether they are published or not. The documents may come from teaching and research institutions in France or abroad, or from public or private research centers.

L'archive ouverte pluridisciplinaire **HAL**, est destinée au dépôt et à la diffusion de documents scientifiques de niveau recherche, publiés ou non, émanant des établissements d'enseignement et de recherche français ou étrangers, des laboratoires publics ou privés.

AUTHOR QUERY FORM

	Journal: J. Chem. Phys. Article Number: JCP24-AR-00154	Please provide your responses and any corrections by annotating this PDF and uploading it to AIP's eProof website as detailed in the Welcome email.
---	---	---

Dear Author,

Below are the queries associated with your article. Please answer all of these queries before sending the proof back to AIP.

Article checklist: In order to ensure greater accuracy, please check the following and make all necessary corrections before returning your proof.

1. Is the title of your article accurate and spelled correctly?
2. Please check affiliations including spelling, completeness, and correct linking to authors.
3. Did you remember to include acknowledgment of funding, if required, and is it accurate?

Location in article	Query/Remark: click on the Q link to navigate to the appropriate spot in the proof. There, insert your comments as a PDF annotation.
Q1	A second proof has been sent to you for confirmation purposes only. At this time, we cannot accept new corrections unless it is to fix an error made by AIP Publishing. When we receive your confirmation, your article will be readied for online publication.

Thank you for your assistance.

First detection and absolute transition frequencies in the (3–0) band of D₂

Cite as: J. Chem. Phys. 160, 000000 (2024); doi: 10.1063/5.0196903

Submitted: 10 January 2024 • Accepted: 16 February 2024 •

Published Online: 9 99 9999



S. Kassi, H. Fleurbaey, and A. Campargue^{a)}

AFFILIATIONS

University Grenoble Alpes, CNRS, LIPhy, 38000 Grenoble, France

^{a)} Author to whom correspondence should be addressed: alain.campargue@univ-grenoble-alpes.fr

ABSTRACT

Three electric quadrupole transitions in the second overtone band of D₂ are newly measured by comb-referenced cavity ring down spectroscopy around 1.18 μm. These extremely weak transitions (line intensities smaller than 10⁻²⁹ cm/molecule) are the first to be detected in the (3–0) band of D₂. The spectra of the O(3), O(2), and Q(2) lines near 8321, 8446, and 8607 cm⁻¹, respectively, are recorded at room temperature for pressure values ranging between 100 and 600 Torr. Accurate transition frequencies and line intensities of the three D₂ transitions are determined from a line fitting procedure using beyond-Voigt profiles, including strong Dicke narrowing. Considering statistical fit errors and possible biases due to the interference with water lines (which are six orders of magnitude stronger than the studied D₂ lines), total uncertainties on the frequencies extrapolated at zero pressure are estimated below 14 MHz (~4.7 × 10⁻⁴ cm⁻¹). The derived experimental frequencies and intensities are compared to *ab initio* values. An overall agreement is achieved, confirming the positional accuracy of the most advanced theoretical calculations.

Published under an exclusive license by AIP Publishing. <https://doi.org/10.1063/5.0196903>

I. INTRODUCTION

The present contribution contributes to the recent efforts of several groups to implement state-of-the-art metrological techniques to determine with very high accuracy the transition frequencies of the hydrogen molecule (H₂) and its deuterated isotopologues (HD, D₂). Being the simplest neutral molecular system, molecular hydrogen allows for sophisticated *ab initio* calculations, including relativistic and quantum electrodynamic (QED) corrections, leading to accuracy on the calculated transition frequencies^{1–5} approaching that of the most advanced experimental setups. In this constructive interplay, the D₂ species is not the most favorable isotopologue for an experimental determination of transition frequencies at high accuracy. Indeed, the D₂ absorption spectrum consists of very weak electric quadrupole (E2) vibrational bands, which are significantly weaker than in H₂. Hydrogen deuteride (HD) is generally preferred for metrological measurements because it shows stronger absorption bands than H₂. This is due to the small charge asymmetry existing in HD, leading to the appearance of a small electric dipole moment. Despite remaining weak, this resulting electric dipole in HD allows E1 transitions which are much stronger than the E2 transitions. Accuracies better than 100 kHz

(i.e., about one thousandth of the room temperature Doppler width) have been recently achieved by several groups for E1 transitions in the first overtone band of HD,^{6–15} where measurements in the saturation regime are feasible. Overall accuracies on HD transition frequencies achieved in saturation regime^{6,8–10,14} are similar to those achieved by state-of-the-art measurements in the Doppler regime,^{12,13} in particular at low temperatures.¹⁵ Up until very recently, H₂ transition frequencies referenced to an absolute frequency standard were practically missing. In the past year, several studies have been dedicated to H₂: the Q1 (1–0) transition frequency was determined with an uncertainty of 310 kHz using stimulated Raman scattering metrology;¹⁶ the Q1–Q4, S0, and S1 transitions of the (2–0) band were reported with uncertainties between a few tens of kHz and 3 MHz by comb referenced cavity ring-down spectroscopy (CR-CRDS) in the Doppler regime;¹⁷ and the S0 transition of the (2–0) band was determined with an accuracy of 8 kHz in the saturation regime using the NICE-OHMS technique under cryogenic conditions.¹⁸

Figure 1 presents an overview of the calculated D₂ spectrum,¹⁹ where the transitions corresponding to the most accurate frequency measurements have been highlighted. The measurements referenced

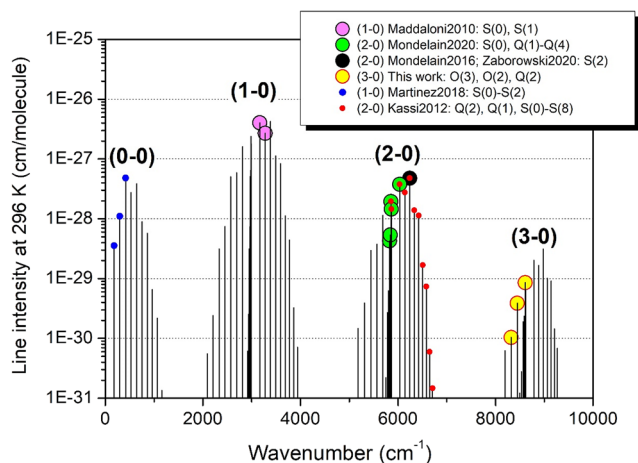


FIG. 1. Overview of the calculated spectrum of D_2 .¹⁹ The literature measurements referenced to an absolute frequency standard from Maddaloni *et al.* (2010),²⁰ Mondelain *et al.* (2016),²¹ Mondelain *et al.* (2020),²⁴ and Zaborowski *et al.* (2020)²³ are plotted with large dots (yellow dots correspond to the present study). Small blue and red dots correspond to the measurements of Ref. 25 [Martínez *et al.* (2019)] and Ref. 19 [Kassi *et al.* (2012)] in the (0–0) and (2–0) bands, respectively.

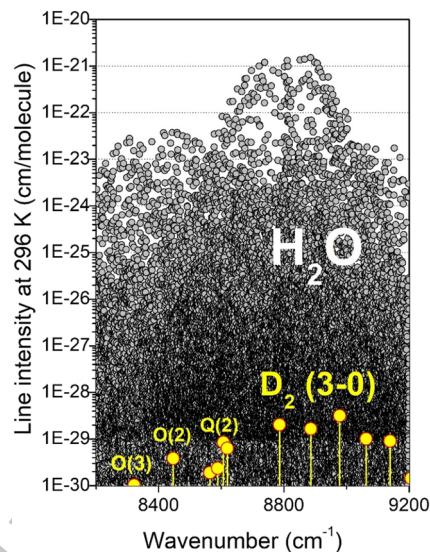


FIG. 2. Calculated spectrum of the (3–0) band of D_2 ¹⁹ superimposed on the spectrum of water vapor.²⁶ The line intensities are for the pure species at 296 K. The assignment of the three D_2 lines under study is indicated.

to an absolute frequency standard are plotted with large dots and include the following: (i) CR-CRDS measurements of the frequencies of the S0 and S1 transitions of the (1–0) fundamental band near $3 \mu\text{m}$, reported with a 6 MHz accuracy using a DFG source referenced to a Cs-clock primary standard via an optical frequency comb synthesizer;²⁰ (ii) the S2 (2–0) transition frequency near 6204 cm^{-1} ($1.61 \mu\text{m}$) measured in our laboratory and Torun with sub-MHz accuracy using CR-CRDS²¹ and frequency-stabilized CRDS in the frequency agile, rapid scanning spectroscopy (FARS) mode,^{22,23} respectively; (iii) the CR-CRDS frequencies of the (2–0) Q1–Q4 and S0 transitions with total uncertainties on the frequencies extrapolated at zero pressure estimated between 0.30 and 1.83 MHz.²⁴ Let us mention that the Q2, Q1, and S0–S8 transitions (small red dots in Fig. 1) were measured in 2012 using standard CRDS,¹⁹ but due to the absence of an absolute reference standard to calibrate the frequency axis, the transition frequencies were reported with an accuracy limited to 30 MHz; (iv) finally, we have highlighted in Fig. 1 the S0–S2 (0–0) rotational transitions (small blue dots) measured by Raman spectroscopy with ± 14 MHz accuracy limited by the used wavemeters.²⁵

The particular weakness of the (3–0) transitions under study (line intensity smaller than $10^{-29} \text{ cm/molecule}$) is a major limitation achieving a high accuracy on the transition frequency. The determination of the transition frequencies requires correcting the pressure-induced line shift in order to extrapolate the line center at the zero pressure limit. Obviously, this extrapolation is more accurate when spectra with good signal-to-noise ratios can be recorded at low pressure [e.g., a few Torr in the case of the Q1, S0, and S1 (2–0) lines of Ref. 17]. In the present case, minimum pressure values of 100 Torr had to be used, which impacts the final transition frequency accuracy. It is worth remembering that Dicke narrowing and speed-dependent effects are exceptionally pronounced in the case of H_2 , HD, and D_2 transitions, and

beyond-Voigt profiles are required to reproduce the measured line profiles, even for spectra having a limited signal-to-noise ratio. Here, we will use the Nelkin–Ghatak profile in the forthcoming analysis.

An additional important contribution to the error budget of the transition frequencies of the three (3–0) transitions measured in this work is related to the interference with water lines. As illustrated in Fig. 2, in the considered region, absorption transitions of water vapor are six orders of magnitude stronger than the targeted D_2 transitions. The use of a flow of D_2 helped to decrease the water vapor absorption, but even with a concentration limited to a few tens of ppm, the superposition with the interfering water lines remained important (see below).

II. EXPERIMENTAL SETUP AND SPECTRA RECORDINGS

The room temperature absorption spectrum of pure D_2 (Aldrich, chemical purity of 99.999% with atomic deuterium isotopic abundance of 99.96%) was recorded in the flow regime by high sensitivity frequency comb referenced cavity ring-down spectroscopy.²¹ The CR-CRDS method and setup used for the recordings have been described in detail in Refs. 24, 27, and 28. The accurate frequency values associated “on the fly” with each ring-down event allow not only an absolute calibration of the frequency axis but also a reduction of the noise amplitude, in particular on the sharp slopes of the line profiles.^{29,30}

The recording procedure is similar to that adopted to measure H_2 transitions in the (2–0) band.¹⁷ An external cavity diode laser (ECDL) is used as a light source. The ECDL (Toptica fiber-connected DL Pro, 1200 nm) was tuned to record small spectral intervals around the O3, O2, and Q2 transitions near 8321 , 8446 , and 8607 cm^{-1} , respectively. The ring-down time τ_0 for the evacuated cavity varied from about 220 to 350 μs , depending on the

wavenumber. For each frequency point, about 50–120 ring-downs were averaged, leading to a minimum detectable absorption coefficient between 3×10^{-12} and 8×10^{-12} cm^{-1} for a single scan. As in Refs. 24, 28, and 29, the frequency calibration of the spectra relied on a self-referenced frequency comb (Model FC 1500-250 WG from Menlo Systems). The frequency corresponding to each ring-down event was determined from (i) the frequency measurement of the beat note between a fraction of the ECDL light and a tooth of the frequency comb and (ii) the tooth number deduced from the frequency value provided by a commercial Fizeau type wavemeter (HighFinesse WSU7-IR, 5 MHz resolution, 20 MHz accuracy over 10 h). For each frequency step, the average central emission frequency of the ECDL was actively stabilized using a software-based proportional-integral loop with a 100 Hz band-pass acting on the laser current.

As mentioned above, in order to minimize the concentration of water vapor desorbing from the CRDS cell or the injection tubes, the spectra were recorded in the flow regime. Nonetheless, strong water lines were apparent in the spectra, and allowing us to estimate the water concentration in the cell to typically be a few tens of ppm. A continuous gas flow of a few sccm was set by slowly pumping the cell through a manual needle valve connecting the cell to a turbo pump group. The gas pressure in the CRDS cell was continuously monitored by a capacitance gauge (MKS Baratron, 1000 mbar full range) and actively regulated by injecting the D_2 sample into the cell through an electro-valve controlled by a computer based proportional/integral loop. For the O_2 line, the recordings were performed at pressure values of 100, 200, 400, and 600 Torr, while a single pressure value of 200 Torr was used for the O3 and Q2 transitions. The spectra in the O2 region are superimposed in Fig. 3. The self-induced pressure shift of the line center and the narrowing of the profile at

higher pressure are observed. The strong nearby line of water vapor near 8446.9 cm^{-1} has an intensity of about 3.7×10^{-24} $\text{cm}/\text{molecule}$, i.e., six orders of magnitude larger than the O_2 line intensity. The contrast between the broadening of the water lines with pressure and the narrowing of the D_2 line is striking. From the relative area of water lines compared to the D_2 line, one can conclude that the relative amount of water vapor clearly varies with pressure. The temperature was measured with a temperature sensor (TSIC 501, 0.1 K accuracy) and varied between 294.7 and 295.4 K, according to the recordings.

III. DATA ANALYSIS AND UNCERTAINTY BUDGET

As mentioned earlier, the standard Voigt profile is not sufficient to adequately model the recorded line profiles due to the prevalence of narrowing effects, requiring the use of more sophisticated line shapes. The Nelkin–Ghatak profile (NGP) accounting for the Dicke effect was found sufficient to account for the recorded line profiles. The fitting program MATS³¹ developed at NIST was used to fit the following parameters of the NGP profile to the spectra: line center, line intensity (extrapolated at 296 K using the lower state energy provided in the HITRAN database²⁶), broadening coefficient (γ_0), and the velocity-changing collision parameter (ν_{VC}) in the hard-collision model. The baseline of each spectrum (typically 1 cm^{-1} wide) was adjusted as a linear function of the wavenumber. During the fitting process, it appeared that the prevalence of narrowing effects and the correlation between the γ_0 and ν_{VC} parameters²² made it difficult to obtain reliable values of the broadening coefficient, in particular for the low pressure recordings (100 and 200 Torr). We thus chose to fix the broadening coefficient of all the lines to the value obtained from the fit of the O_2 line profile at 600 Torr. The adopted $5.0 \times 10^{-3} \text{ cm}^{-1} \text{ atm}^{-1}$ default value is consistent with the $4\text{--}8 \times 10^{-3} \text{ cm}^{-1} \text{ atm}^{-1}$ range of the γ_0 values obtained for the S0, Q1–Q4 lines of the (2–0) band.²⁴

All spectra are affected by interference from strong water lines due to outgassing (see Figs. 2 and 4). In the analysis, for the strongest water lines, the NGP profile was used, and the corresponding γ_0 and ν_{VC} parameters were floated while positions and intensities were fixed to parameters from the HITRAN database.²⁶ Weaker water lines were simulated as Voigt profiles using HITRAN parameters. The water mole fraction was fit during the analysis and found to vary between ~ 10 and 100 ppm, well beyond the sub-ppm amount stated in the gas sample. Note that, due to exchanges between D_2 and water vapor, water vapor is strongly enriched in deuterium, and the relative concentration of HDO, which was also floated, exceeds its natural value by typically a factor of 30.

The derived line parameters are listed in Table I.

We have included in Fig. 3 the (meas. - calc.) residuals from the fits of the O_2 line. In the region of the D_2 line, the spectra are reproduced at the noise level (typically about $5 \times 10^{-12} \text{ cm}^{-1}$). The residuals corresponding to all three lines at 200 Torr are presented in Fig. 4. The individual contributions of the water interfering lines can be assessed from this figure, where the individual line profiles are

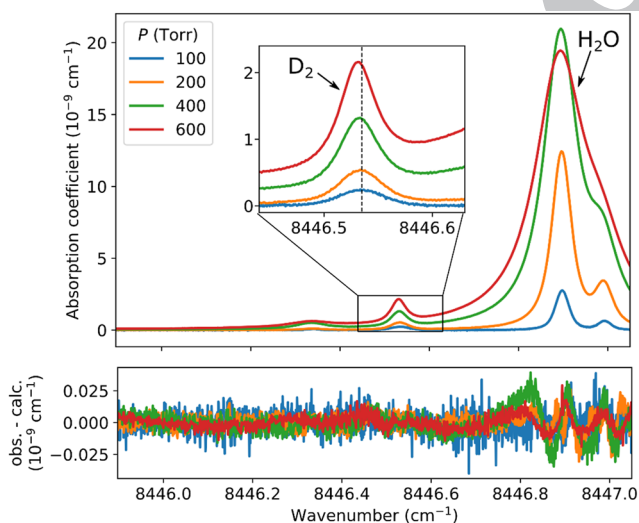


FIG. 3. Comparison of the spectra in the region of the (3–0) O_2 D_2 line recorded at different pressures (100, 200, 400, and 600 Torr). Note the narrowing of the D_2 line profile at higher pressure, while water lines show a strong pressure broadening. The insert shows the pressure variation of the D_2 line profile, in particular the pressure shift compared to the zero-pressure position (dashed vertical line). The lower panel shows the residuals from the fits.

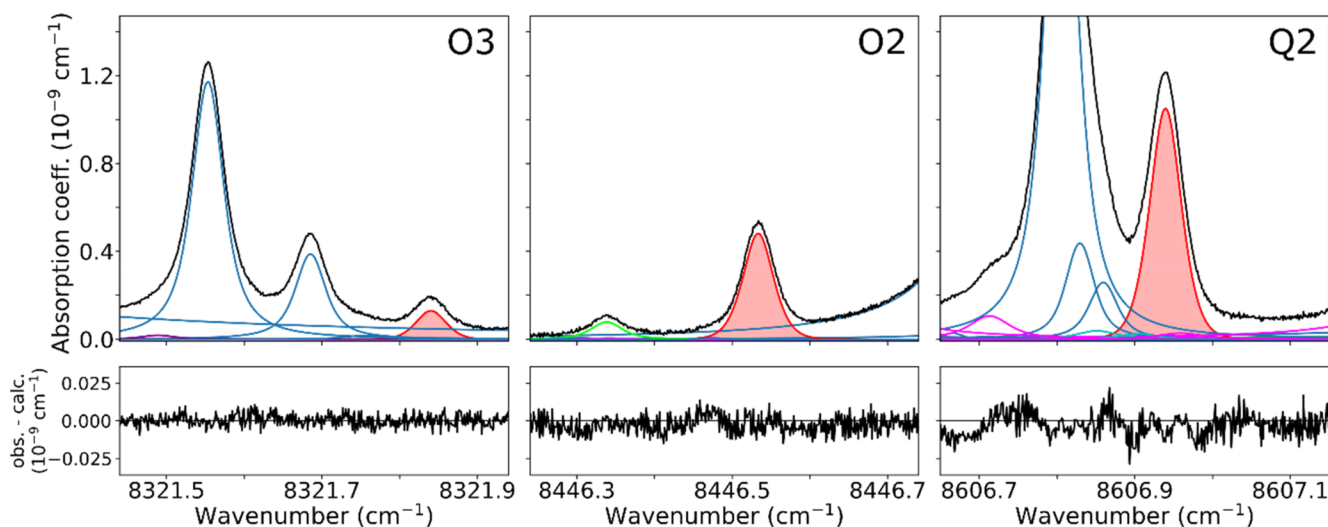


FIG. 4. Spectra of the (3–0) O3, O2, and Q2 D₂ lines recorded at 200 Torr. The upper panels present the experimental spectra and the best fit obtained with NGP profiles for the D₂ line and the interfering water lines (H₂¹⁶O: blue profiles, H₂¹⁸O: cyan, H₂¹⁷O: purple, and HDO: magenta). An interfering line of NH₃ is also visible in the middle panel around 8446.3 cm⁻¹ (green profile). The D₂ lines are highlighted with filled-in red profiles. The corresponding residuals are presented on the lower panels.

TABLE I. Parameters of the (3–0) O3, O2, and Q2 transitions of D₂ obtained at different pressures using a NGP profile.

Transition	<i>P</i> (Torr)	Position ^a (cm ⁻¹)	<i>S</i> (296 K) ^{a,b} (10 ⁻³⁰ cm/molecule)	<i>v</i> _{VC} ^{a,c} (10 ⁻³ cm ⁻¹ atm ⁻¹)
O3	200	8321.840 18(16)	1.034(18)	23.4(25)
O2	100	8446.534 13(15)	4.019(22)	17.5(27)
	200	8446.533 35(11)	3.912(50)	21.0(16)
	400	8446.532 14(8)	3.889(38)	22.5(8)
	600	8446.530 95(4)	3.847(24)	23.2(4)
Q2	200	8606.939 56(6)	8.843(78)	18.2(11)

^aThe uncertainties are given within parentheses in the unit of the last quoted digit and include the (1 σ) statistical values provided by the fit and potential biases related to the spectrum baseline and water interfering lines (see the text).

^bThe intensity values are given for a reference temperature of 296 K.

^cThe pressure broadening coefficient (γ_0) of all the lines was fixed to a default value of 5.0×10^{-3} cm⁻¹ atm⁻¹ (see the text).

displayed (red and blue profiles for D₂ and H₂¹⁶O, respectively, with magenta for HDO). The O2 line appears to be the most affected.

The error bars given in Table I include the statistical uncertainty of the fits and the error bars related to the spectrum baseline and to the interfering lines. To evaluate these last two, we investigated the influence of a change of $\pm 1\%$ in the water vapor concentrations; this variation corresponds to a mismatch of the concentration clearly visible in the residuals. Similarly, we estimated the impact of the baseline by varying the spectral range over which the fit was performed. The resulting combined error bars are in the position range between 4×10^{-5} and 1.6×10^{-4} cm⁻¹ (1.2 and 4.8 MHz, respectively). For the high-pressure recordings of the O2 line, the uncertainty related to the interfering lines is maximum: for the line positions, it is comparable to the fit uncertainty, while it is the main error source for the line intensities.

IV. COMPARISON WITH *AB INITIO* CALCULATIONS

For comparison to *ab initio* positions, the measured line positions have to be extrapolated to zero-pressure. The significance of the self-pressure shift is illustrated in the insert included in Fig. 3. A linear regression of the O2 line positions as a function of pressure yields the zero-pressure position and the self-pressure shift (Fig. 5). In the case of the H₂ lines, it was observed that the pressure shift (δ_0) becomes non-linear with pressure as the pressure increases above 200 Torr.^{17,32,33} We observe a very similar behavior, with the pressure shift at low pressure being slightly larger than at high pressure (see Fig. 2 of Ref. 33 and Fig. 4 of Ref. 17 for comparison). The zero-pressure O2 position obtained from the 100 and 200 Torr positions is 8446.534 91(38) cm⁻¹, with the error bar being the maximum value calculated from the experimental uncertainties given in Table I. Including the measurements at 400 and 600 Torr leads to a decrease

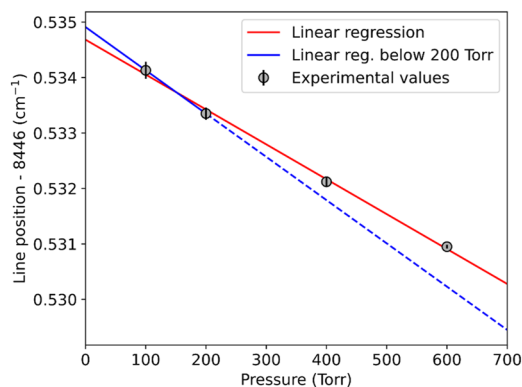


FIG. 5. Linear regressions of the line position of the O2 line as a function of pressure to extract the zero-pressure position. The plotted blue and red lines correspond to the linear regressions obtained with the 100 and 200 Torr positions and with the whole set of measured positions between 100 and 600 Torr, respectively.

in the zero-pressure position by $2.3 \times 10^{-4} \text{ cm}^{-1}$ (or 6.8 MHz) and a 24% variation of the pressure induced shift ($-4.8 \times 10^{-3} \text{ cm}^{-1} \text{ atm}^{-1}$ instead of $-5.9 \times 10^{-3} \text{ cm}^{-1} \text{ atm}^{-1}$). For the O3 and Q2 transitions, the zero pressure position was obtained by adopting the low pressure δ_0 value of the O2 line. This choice is supported by the limited rotational dependence of the δ_0 values obtained for the S0, Q1–Q4 lines of the (2–0) band (from -2.99×10^{-3} to $-2.53 \times 10^{-3} \text{ cm}^{-1} \text{ atm}^{-1}$).²⁴

A reliable evaluation of the uncertainties in the resulting zero pressure positions is difficult. According to the O2 data at disposal, a value of 12 MHz ($4 \times 10^{-4} \text{ cm}^{-1}$) seems to be a conservative estimate of the error related to the position extrapolation at zero-pressure. This value is larger than the measurement uncertainty on the O3 position at 200 Torr ($1.6 \times 10^{-4} \text{ cm}^{-1}$), leading to a combined uncertainty of $4.3 \times 10^{-4} \text{ cm}^{-1}$ (12.9 MHz) for this line. In the case of the Q2 line, the uncertainty is dominated by the zero-pressure extrapolation of the line center, leading to a 12 MHz estimated error bar. In summary, the main source of uncertainty on the line position is related to the zero-pressure extrapolation, which leads to a similar error bar of $4 \times 10^{-4} \text{ cm}^{-1}$ or 12 MHz for the three measured lines.

In Table II, we have gathered the positions and intensities and their final uncertainties, obtained in this work, with the corresponding values predicted by theory. The table includes the *ab initio* position values and uncertainties provided by the H₂ Spectre computer code.³⁴ It is worth pointing out that most (3–0) D₂ *ab initio* transition frequencies have an uncertainty (1σ) of 14 MHz ($4.7 \times 10^{-4} \text{ cm}^{-1}$) similar to our average experimental uncertainty, but the O2 transition reaching the $J = 0$ upper rotational level is calculated with a much higher accuracy of 0.95 MHz ($3 \times 10^{-5} \text{ cm}^{-1}$). The (exp. - calc.) position differences included in Table II range between +3.6 and 13.0 MHz, well below the combined error bars of the experimental and *ab initio* transition frequencies.

Finally, the intensity comparison between the experiment and theory included in Table II shows agreement within about 3%, which should be considered satisfactory considering the weakness of the considered transitions and the interference with the water lines.

V. CONCLUSION

The first detection of electric quadrupole transitions in the second overtone band of D₂ has been achieved by comb-referenced cavity ring down spectroscopy near 1.18 μm . With line intensities in the 10^{-30} – $10^{-29} \text{ cm}^2/\text{molecule}$ range, the studied transitions (O2, O3, and Q2) are among the weakest absorption lines measured so far. The Nelkin–Ghatak profile, accounting for strong collisional narrowing effects, was used to fit the different line profiles measured for pressure values ranging between 100 and 600 Torr. The absolute frequency of the O2, O3, and Q2 transitions was obtained with a claimed accuracy of about 12 MHz, mainly determined by the error bar on the zero pressure extrapolation of the line centers. This uncertainty value corresponds to less than 1% of the room temperature Doppler width (1.55 GHz, FWHM) and is only twice as large as that achieved for the three orders of magnitude stronger S0 and S1 transitions of the (1–0) fundamental band.²⁰

Except for the O2 (3–0) transition computed with a 0.95 MHz error bar, the (3–0) *ab initio* transition frequencies are provided with an uncertainty similar to our experimental uncertainty (≈ 14 MHz). A good agreement (better than 13 MHz) is obtained between the measured and *ab initio* position values. Sub-MHz determinations of transition frequencies in D₂ are available only in the (2–0) band,^{22–24} in particular for the S2 transition, which is about 50 times stronger than the O2 (3–0) transition (see Fig. 1). This level of accuracy

TABLE II. Center, intensity for the O3, O2, and Q2 transitions of the (3–0) band of D₂ and comparison to the calculated values.

Transition	Position (cm^{-1})				Intensity at 296 K ($10^{-30} \text{ cm}^2/\text{molecule}$)		
	Experimental	<i>Ab initio</i> ^a	Exp.-calc.		Experimental	<i>Ab initio</i> ^b	Exp./calc.
			10^{-5} cm^{-1}	MHz			
O3	8321.841 73(43)	8321.841 48(47)	25	7.6	1.034(18)	1.032	1.002
O2	8446.534 91(38)	8446.534 79(3)	12	3.6	3.911(59)	3.855	1.014
Q2	8606.941 11(40)	8606.940 68(47)	43	13.0	8.843(78)	8.548	1.034

^a*Ab initio* position values provided by the H2Spectre software.^{2,34}

^b*Ab initio* intensity values from Ref. 19.

revealed a slight underestimation of the *ab initio* transition frequencies in the (2–0) band, on the order of 1.6 MHz in the case of the S2 (2–0) transition, about twice the calculated error bar. Note that this situation is very similar to that found in the (2–0) band of HD and H₂: calculated frequencies are systematically underestimated by 1.6 and 1.1 MHz, respectively (corresponding to about 1.7 times their claimed uncertainties) compared to a series of measurements with an accuracy of a few tens of kHz.¹⁷

As concerns the (3–0) band of D₂, a significant reduction of the experimental uncertainty should be possible for the S0 and S2 transitions near 8786 and 8978 cm⁻¹, respectively. These transitions are the strongest of the (3–0) band (see Fig. 2), which will allow using lower pressure recordings and, thus, improve the accuracy on the line center at zero pressure. These future metrological measurements, together with the present work, will provide additional validation tests of the state-of-the-art *ab initio* calculations of molecular levels of hydrogen isotopologues, with a possible impact on fundamental physics.^{35–37}

ACKNOWLEDGMENTS

This project was supported by the REFIMEVE consortium (Grant No. Equipex REFIMEVE+ANR-11-EQPX-0039). Valuable communications with J. Komasa (Poznan), K. Pachucki (Warsaw), W. Ubachs (Amsterdam), and M. L. Diouf (Amsterdam) about the *ab initio* values of the D₂ transition frequencies are acknowledged.

AUTHOR DECLARATIONS

Conflict of Interest

The authors have no conflicts to disclose.

Author Contributions

S. Kassi: Investigation (lead); Methodology (lead); Writing – original draft (lead); Writing – review & editing (lead). **H. Fleurbaey:** Formal analysis (lead); Investigation (lead); Methodology (lead); Writing – review & editing (equal). **A. Campargue:** Formal analysis (lead); Writing – original draft (lead); Writing – review & editing (lead).

DATA AVAILABILITY

The data that support the findings of this study are available from the corresponding author upon reasonable request.

REFERENCES

- ¹P. Czachorowski, M. Puchalski, J. Komasa, and K. Pachucki, “Nonadiabatic relativistic correction in H₂, D₂, and HD,” *Phys. Rev. A* **98**, 052506 (2018).
- ²J. Komasa, M. Puchalski, P. Czachorowski, G. Łach, and K. Pachucki, “Rovibrational energy levels of the hydrogen molecule through nonadiabatic perturbation theory,” *Phys. Rev. A* **100**, 032519 (2019).
- ³M. Puchalski, A. Spyszkiwicz, J. Komasa, and K. Pachucki, “Nonadiabatic relativistic correction to the dissociation energy of H₂, D₂, and HD,” *Phys. Rev. Lett.* **121**, 073001 (2018).

- ⁴M. Puchalski, J. Komasa, A. Spyszkiwicz, and K. Pachucki, “Dissociation energy of molecular hydrogen isotopologues,” *Phys. Rev. A* **100**, 020503 (2019).
- ⁵E. Roueff, H. Abgrall, P. Czachorowski, K. Pachucki, M. Puchalski, and J. Komasa, “The full infrared spectrum of molecular hydrogen,” *Astron. Astrophys.* **630**, A58 (2019).
- ⁶F. M. J. Cozijn, P. Dupré, E. J. Salumbides, K. S. E. Eikema, and W. Ubachs, “Sub-Doppler frequency metrology in HD for tests of fundamental physics,” *Phys. Rev. Lett.* **120**, 153002 (2018).
- ⁷F. M. J. Cozijn, M. L. Diouf, V. Hermann, E. J. Salumbides, M. Schlösser, and W. Ubachs, “Rotational level spacings in HD from vibrational saturation spectroscopy,” *Phys. Rev. A* **105**, 062823 (2022).
- ⁸M. L. Diouf, F. M. J. Cozijn, B. Darquié, E. J. Salumbides, and W. Ubachs, “Lamb-dips and lamb-peaks in the saturation spectrum of HD,” *Opt. Lett.* **44**, 4733 (2019).
- ⁹M. L. Diouf, F. M. J. Cozijn, K.-F. Lai, E. J. Salumbides, and W. Ubachs, “Lamb-peak spectrum of the HD (2–0) P(1) line,” *Phys. Rev. Res.* **2**, 023209 (2020).
- ¹⁰T.-P. Hua, Y. R. Sun, and S.-M. Hu, “Dispersion-like lineshape observed in cavity-enhanced saturation spectroscopy of HD at 1.4 μm,” *Opt. Lett.* **45**, 4863 (2020).
- ¹¹A. Fast and S. A. Meek, “Sub-ppb measurement of a fundamental band rovibrational transition in HD,” *Phys. Rev. Lett.* **125**, 023001 (2020).
- ¹²A. Castrillo, E. Fasci, and L. Gianfrani, “Doppler-limited precision spectroscopy of HD at 1.4 μm: An improved determination of the R(1) center frequency,” *Phys. Rev. A* **103**, 022828 (2021).
- ¹³A. Castrillo, E. Fasci, and L. Gianfrani, “Erratum: Doppler-limited precision spectroscopy of HD at 1.4 μm: An improved determination of the R(1) center frequency [Phys. Rev. A 103, 022828 (2021)],” *Phys. Rev. A* **103**, 069902 (2021).
- ¹⁴M. L. Niu, E. J. Salumbides, G. D. Dickenson, K. S. E. Eikema, and W. Ubachs, “Precision spectroscopy of the X¹Σg⁺, v = 0 → 1 (J = 0–2) rovibrational splittings in H₂, HD and D₂,” *J. Mol. Spectrosc.* **300**, 44 (2014).
- ¹⁵S. Kassi, C. Lauzin, J. Chaillot, and A. Campargue, “The (2–0) R(0) and R(1) transition frequencies of HD determined to a 10⁻¹⁰ relative accuracy by Doppler spectroscopy at 80 K,” *Phys. Chem. Chem. Phys.* **24**, 23164 (2022).
- ¹⁶M. Lamperti, L. Rutkowski, D. Ronchetti *et al.*, “Stimulated Raman scattering metrology of molecular hydrogen,” *Commun. Phys.* **6**, 67 (2023).
- ¹⁷H. Fleurbaey, A. O. Koroleva, S. Kassi, and A. Campargue, “The high-accuracy spectroscopy of H₂ rovibrational transitions in the (2–0) band near 1.2 μm,” *Phys. Chem. Chem. Phys.* **25**(21), 14749–14756 (2023).
- ¹⁸F. M. J. Cozijn, M. L. Diouf, and W. Ubachs, “Lamb dip of a quadrupole transition in H₂,” *Phys. Rev. Lett.* **131**, 073001 (2023).
- ¹⁹S. Kassi, A. Campargue, K. Pachucki, and J. Komasa, “The absorption spectrum of D₂: Ultrasensitive cavity ring down spectroscopy of the (2–0) band near 1.7 μm and accurate *ab initio* line list up to 24000 cm⁻¹,” *J. Chem. Phys.* **136**, 184309 (2012).
- ²⁰P. Maddaloni, P. Malara, E. De Tommasi, M. De Rosa, I. Ricciardi, G. Gagliardi, F. Tamassia, G. Di Lonardo, and P. De Natale, “Absolute measurement of the S(0) and S(1) lines in the electric quadrupole fundamental band of D₂ around 3 μm,” *J. Chem. Phys.* **133**, 154317 (2010).
- ²¹D. Mondelain, S. Kassi, T. Sala, D. Romanini, D. Gatti, and A. Campargue, “Sub-MHz accuracy measurement of the S(2) 2–0 transition frequency of D₂ by comb-assisted cavity ring down spectroscopy,” *J. Mol. Spectrosc.* **326**, 5–8 (2016).
- ²²P. Wcislo, F. Thibault, M. Zaborowski, S. Wójtewicz, A. Cygan, G. Kowzan, P. Masłowski, J. Komasa, M. Puchalski, K. Pachucki, R. Ciuryło, and D. Lisak, “Accurate deuterium spectroscopy for fundamental studies,” *J. Quant. Spectrosc. Radiat. Transfer* **213**, 41–51 (2018).
- ²³M. Zaborowski, M. Słowinski, K. Stankiewicz, F. Thibault, A. Cygan, H. Józwiak, G. Kowzan, P. Masłowski, A. Nishiyama, N. Stolarczyk, S. Wójtewicz, R. Ciuryło, D. Lisak, and P. Wcislo, “Ultrahigh finesse cavity-enhanced spectroscopy for accurate tests of quantum electrodynamics for molecules,” *Opt. Lett.* **45**, 1603–1606 (2020).
- ²⁴D. Mondelain, S. Kassi, A. Campargue, and A. Campargue, “Transition frequencies in the (2–0) band of D₂ with MHz accuracy,” *J. Quant. Spectrosc. Radiat. Transfer* **253**, 107020 (2020).
- ²⁵R. Z. Martínez, D. Bermejo, P. Wcislo, and F. Thibault, “Accurate wavenumber measurements for the S0(0), S0(1), and S0(2) pure rotational Raman lines of D₂,” *J. Raman Spectrosc.* **50**, 127–129 (2019).

- 462 ²⁶I. E. Gordon, L. S. Rothman, R. J. Hargreaves, R. Hashemi, E. V. Karlovets
463 *et al.*, “The HITRAN 2020 molecular spectroscopic database,” *J. Quant. Spectrosc.*
464 *Radiat. Transfer* **277**, 107949 (2021).
- 465 ²⁷D. Mondelain, T. Sala, S. Kass, D. Romanini, M. Marangoni, and A. Campargue,
466 “Broadband and highly sensitive comb-assisted cavity ring down spectroscopy of CO near 1.57 μm with sub-MHz frequency accuracy,” *J. Quant. Spectrosc. Radiat. Transfer* **154**, 35–43 (2015).
- 469 ²⁸B. Bordet, S. Kass, and A. Campargue, “Line parameters of the 4-0 band of carbon monoxide by high sensitivity cavity ring down spectroscopy near 1.2 μm ,” *J. Quant. Spectrosc. Radiat. Transfer* **260**, 107453 (2021).
- 472 ²⁹M. Konefal, S. Kass, D. Mondelain, and A. Campargue, “High sensitivity spectroscopy of the O₂ band at 1.27 μm : (I) pure O₂ line parameters above 7920 cm^{-1} ,” *J. Quant. Spectrosc. Radiat. Transfer* **241**, 106653 (2020).
- 475 ³⁰S. Vasilchenko, H. Tran, D. Mondelain, S. Kass, and A. Campargue, “Accurate absorption spectroscopy of water vapor near 1.64 μm in support of the Methane Remote Lidar mission (MERLIN),” *J. Quant. Spectrosc. Radiat. Transfer* **235**, 332–342 (2019).
- ³¹E. M. Adkins, “MATS, Multi-spectrum Analysis Tool for Spectroscopy,” 2020. 479
- ³²P. Wcislo, I. E. Gordon, H. Tran, Y. Tan, S.-M. Hu, A. Campargue, S. Kass, D. Romanini, C. Hill, R. V. Kochanov, and L. S. Rothman, “The implementation of non-Voigt line profiles in the HITRAN database: H₂ case study,” *J. Quant. Spectrosc. Radiat. Transfer* **177**, 75–91 (2016). 480
481
482
483
- ³³P. Wcislo, I. E. Gordon, C.-F. Cheng, S.-M. Hu, and R. Ciurylo, “Collision-induced lineshape effects limiting the accuracy in Doppler-limited spectroscopy of H₂,” *Phys. Rev. A* **93**, 022501 (2016). 484
485
486
- ³⁴H2Spectre version 7.4, Fortran source code, available at <https://qcg.home.amu.edu.pl/H2Spectre.html>, University of Warsaw, Poland, 2022. 487
488
- ³⁵F. Heiße, F. Köhler-Langes, S. Rau, J. Hou, S. Junck, A. Kracke *et al.*, “High-precision measurement of the proton’s atomic mass,” *Phys. Rev. Lett.* **119**, 033001 (2017). 489
490
- ³⁶R. Pohl, R. Gilman, G. A. Miller, and K. Pachucki, “Muonic hydrogen and the proton radius puzzle,” *Annu. Rev. Nucl. Part. Sci.* **63**(1), 175–204 (2013). 491
492
- ³⁷W. Ubachs, J. Koelemeij, K. Eikema, and E. Salumbides, “Physics beyond the standard model from hydrogen spectroscopy,” *J. Mol. Spectrosc.* **320**, 1–12 (2016). 493
494